Neuron, Vol. 16, 113–122, January, 1996, Copyright ©1996 by Cell Press

Molecular Basis of Charge Movement in Voltage-Gated Sodium Channels

Naibo Yang,* Alfred L. George, Jr.,† and Richard Horn*
*Department of Physiology
Jefferson Medical College
Philadelphia, Pennsylvania 19107
†Department of Medicine
Department of Pharmacology
Vanderbilt University School of Medicine
Nashville, Tennesee 37232

Summary

Voltage-dependent movement of a sodium channel S4 segment was examined by cysteine scanning mutagenesis and testing accessibility of the residues to hydrophilic cysteine-modifying reagents. These experiments indicate that 2 charged S4 residues move completely from an internally accessible to an externally accessible location in response to depolarization by passage through a short "channel" in the protein. The energetic problems of S4 movement have thus been solved in the same way that many ion channels achieve highly selective and rapid ion permeation through an open pore, by restricting the contact region between the permion and its channel.

Introduction

Voltage-gated sodium, calcium, and potassium channels belong to a superfamily of ubiquitous proteins, all of which are exquisitely sensitive to membrane potential. It is precisely this voltage sensitivity that defines their function, both in the excitable cells of nerve and muscle, and in inexcitable cells such as lymphocytes or kidney cells. To account for this response to voltage, the transition from a resting, closed conformation to an open conformation must be accompanied by the translocation of an equivalent of at least 10 charges across the membrane (Schoppa et al., 1992; Sigworth, 1993; Zagotta et al., 1994; Hirschberg et al., 1995). The postulated structure of the sodium channel consists of a tandem arrangement of four domains (D1–D4), each with six membrane spanning segments (S1–S6) (Noda et al., 1984; Catterall, 1986). Only one type of transmembrane segment, S4, is highly charged, containing 4, 5, 6, and 8 basic residues in D1, D2, D3, and D4, respectively. S4 segments have a unique repetitive structure; every third amino acid is positively charged (either arginine or lysine) and the intervening residues are hydrophobic. The paucity of charges in other putative transmembrane segments makes S4 a natural candidate for the gating voltage sensor. Depolarization is predicted to cause an outward movement of the S4 segments (Catterall, 1986; Durell and Guy, 1992; Sigworth, 1993), leading to the opening of the channels, a process known as activation.

The principal evidence that S4 is the voltage sensor underlying gating is that mutations of both charged and hydrophobic residues within S4 can reduce the voltage dependence of activation and shift the voltage range over which activation occurs (Stühmer et al., 1989; Auld et al., 1990; Liman et al., 1991; Lopez et al., 1991; McCormack et al., 1991; Papazian et al., 1991; Logothetis et al., 1992, 1993; Schoppa et al., 1992; Fleig et al., 1994; Perozo et al., 1994; Papazian et al., 1995). We have recently presented evidence for the outward movement of an S4 segment in response to depolarization of the adult human skeletal muscle sodium channel (hSkM1) (Yang and Horn, 1995). In these experiments, we showed that the outermost basic residue of S4/D4, when changed from arginine to cysteine (D4:R1C), is accessible to extracellular application of the methanethiosulfonate (MTS) reagents methanethiosulfonate-ethyltrimethylammonium (MTSET) and -ethylsulfonate (MTSES) (Akabas et al., 1992; Stauffer and Karlin, 1994) only when the channel is depolarized. The reaction of MTS reagents with the introduced cysteine residue was monitored by following changes in gating kinetics.

The extracellular appearance and disappearance of D4:R1C in response to changes of membrane potential only show that a voltage-dependent conformational transition occurs in the vicinity of S4/D4. This might be expected if S4 segments are intimately associated with the activation gates. The proposition that S4 segments are the voltage sensors for gating remains problematic, however, until several questions are addressed. First, if each S4 segment contributes equally to charge movement, it must be capable of moving the equivalent of at least 2.5 elementary charges across the membrane field. Either a few charged residues must move completely across the membrane field, or else several buried charges each move a smaller electrical distance. Is an S4 segment capable of moving so many residues ($\geq$2.5 basic residues, plus the intervening hydrophobic residues) across the membrane field? Second, in hSkM1 there are 8 basic residues in S4/D4, but only 4 negatively charged residues within putative transmembrane segments in D4 (George et al., 1992). How can so many basic residues be packed into the hydrophobic core of the protein in the absence of countercharges? Third, how is so much charge moved so rapidly and reversibly across the membrane field in the face of apparently large energy barriers due to the hydrophobicity of the protein's core? The answers to these questions are key to understanding the molecular dynamics of gating. We show here that 2 basic S4 residues, and presumably the 2 hydrophobic residues between them, move completely from an inwardly accessible to an outwardly accessible location in response to depolarization, and that the short "channel" through which S4/D4 moves contains at most one basic residue at a time, obviating the need for a large number of countercharges.

Results

Voltage-Dependent Accessibility of S4/D4 Residues

Depolarization exposes D4:R1C to extracellular cysteine reagents (Yang and Horn, 1995). Here, we examine

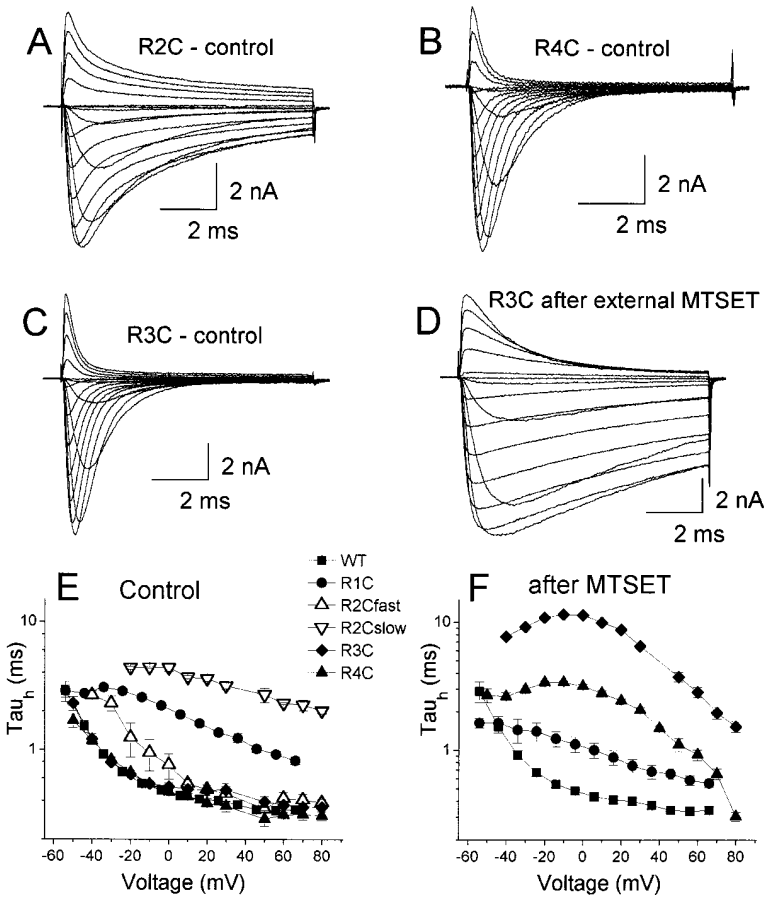

Figure 1. Currents of Cysteine Mutants and Effects of MTSET

(A) Control currents of R2C. $V_{hold} = -140$ mV, 9 ms test pulses from −70 mV to +80 mV in 10 mV increments.

(B) Control R4C currents. Test pulses from −80 mV to +70 mV in 10 mV increments.

(C) Control R3C currents. Same voltages as in (A).

(D) R3C currents (same cell) after 5 min exposure to 100 μM MTSET.

(E and F) Inactivation time constants (τ_h). A fast and slow τ_h were needed for R2C (open symbols). These values were not significantly affected by 500 μM external MTSET and are not shown in (F). All effects are for extracellular application of MTSET except for R4C, which is only sensitive to intracellular MTSET.

whether other basic residues in S4/D4 also show voltage-dependent accessibility to hydrophilic reagents. To this end, we substituted a cysteine for each of the remaining 7 basic residues of S4/D4 of hSkM1; expressed these point mutants (i.e., R2C–R6C, K7C, and R8C) in a mammalian cell line; and examined the effects of cysteine reagents on their sodium currents during whole-cell recording. The inactivation kinetics after a depolarization can be well fit by a single exponential function at each voltage for wild-type (WT) channels and all cysteine mutants except R2C, where a weighted sum of 2 exponentials is required (Figure 1).

The currents of R3C, which have biophysical properties similar to WT channels (Figure 1E; Table 1), are dramatically affected by extracellular MTSET. Figure 1C shows a family of R3C sodium currents elicited by a series of depolarizations in the absence of reagent, and Figure 1D shows currents from the same cell after modification by 100 μM MTSET. Figures 1E and 1F show that inactivation time constants (τ_h) of R3C are increased >10-fold by MTSET and that the voltage dependence of τ_h is also altered. By contrast, the inactivation time constants of R2C and R4C–R8C are not affected by extracellular MTSET (data not shown). The time course of MTSET modification for the cell of Figures 1C and 1D is displayed in Figure 2A. The initial exposure to 100 μM MTSET had no effect on this cell when brief test pulses to −20 mV were applied every 20 s from a holding potential of −140 mV (Figure 2, trace 1). However, when the cell was depolarized during the 20 s intervals between test pulses (a total duration of 9 s at −20 mV during each 20 s interval; see Experimental Procedures), the inactivation kinetics immediately began to change, as a slow component replaced the rapidly inactivating component (Figure 2A). The modification of inactivation kinetics was complete within ~4 min. During the modification, the inactivation kinetics were well fit by a weighted sum of 2 exponentials with a fast time constant representing unmodified channels and a slow time constant representing modified channels. These data show that, like R1C (Yang and Horn, 1995), the residue R3C is accessible to extracellular MTSET only when the channel is depolarized.

To explore the voltage dependence of R3C's accessibility, we measured the rate of modification by 100 μM MTSET for depolarizations to different voltages. Figure 2B shows that the MTSET reaction, estimated from the weight of the slow component of inactivation, has exponential kinetics with a rate that increases with depolarization (see also Figure 2C, closed squares). If R3C exposure is a prerequisite for the reaction with extracellular MTSET, and this exposure is much faster than the reaction rate of 100 μM MTSET, the sigmoidal dependence of the reaction rate with voltage (Figure 2C) represents the scaled steady-state probability of R3C exposure (Yang and Horn, 1995). These data are well fit with a Boltzmann relationship (Figure 2C, solid line), indicating that the exposure of R3C can be described by a first-order voltage-dependent reaction, as we observed previously for R1C (Figure 2C, dashed line). The parameters

Table 1. Boltzman Parameters for Fits to Normalized Conductance–Voltage (G–V) and Steady-State Inactivation Curves and Effects of Cysteine Reagents

	G–V		Steady-State Inactivation	
	Midpoint (mV)	Slope (e_0)	Midpoint (mV)	Slope (e_0)
CONTROL				
WT	−38.2 ± 1.3	3.09 ± 0.18	−88.4 ± 0.4	4.98 ± 0.17
R1C	−39.6 ± 2.0	3.21 ± 0.13	−103.6 ± 1.4	1.88 ± 0.07
R2C	−33.7 ± 2.4	3.06 ± 0.14	−94.5 ± 0.6	3.48 ± 0.15
R3C	−35.1 ± 2.0	3.11 ± 0.11	−100.1 ± 0.6	4.03 ± 0.26
R4C	−31.1 ± 2.2	2.97 ± 0.15	−110.5 ± 3.8	3.94 ± 0.11
R5C	−25.5 ± 3.5	2.35 ± 0.08	−98.8 ± 2.3	2.97 ± 0.12
R6C	−34.7 ± 3.4	3.05 ± 0.10	−94.0 ± 2.4	4.09 ± 0.13
K7C	−33.5 ± 2.2	3.19 ± 0.06	−87.2 ± 2.2	3.75 ± 0.15
R8C	−37.5 ± 2.6	3.14 ± 0.07	−86.8 ± 2.3	3.32 ± 0.18
MTSET				
WT	−36.7 ± 2.1	3.12 ± 0.28	−93.6 ± 2.3	4.42 ± 0.24
R1C	−34.8 ± 3.6	2.76 ± 0.10	−116.3 ± 0.5	2.38 ± 0.09
R3C	−36.2 ± 1.8	3.72 ± 0.07	−79.1 ± 1.3	3.01 ± 0.13
R4C	−40.7 ± 2.8	3.67 ± 0.18	−80.8 ± 2.4	2.94 ± 0.10
MTSES				
R2C	−32.8 ± 4.3	3.41 ± 0.12	−99.5 ± 4.8	2.40 ± 0.39
R5C	−38.3 ± 5.9	2.49 ± 0.32	−103.4 ± 1.2	2.66 ± 0.13
R6C	−38.9 ± 4.1	2.97 ± 0.10	−90.3 ± 1.7	3.50 ± 0.08
K7C	−36.0 ± 1.5	3.09 ± 0.30	−89.4 ± 1.4	3.94 ± 0.50
R8C	−36.4 ± 2.1	3.08 ± 0.19	−90.8 ± 4.4	2.41 ± 0.07

Fits were obtained before and after reagent treatment. For WT, R1C, and R3C, the effects of extracellular 100 μM MTSET are shown, using depolarizations to expose the introduced cysteine residues, when present. For R4C, the effect of intracellular 200 μM MTSET is shown. For all other clones, the effects of intracellular 2 mM MTSES are shown. Slopes are presented as equivalent charge transferred.

of the fit indicate that exposure of R3C involves the movement of an equivalent of 0.96 ± 0.17 elementary charges (e_0) across the membrane, and that the midpoint of this charge movement is −73.8 ± 6.3 mV. The different voltage dependence for exposure of R1C and R3C is expected if these point mutations have unique effects on S4/D4 movement. The lower slope for the R3C mutant (0.96 versus 1.47 e_0) suggests that R3 plays a greater role than R1 on S4/D4 movement. After consideration of the concentration of MTSET, the total durations of depolarizations (9 s depolarized in each 20 s interval), and the maximum estimated rate of R3C modification at depolarized voltages, we calculate a second order rate constant of 778 $M^{-1}s^{-1}$ for the reaction of MTSET with exposed R3C, which is about half the value previously estimated for exposed R1C (Yang and Horn, 1995). These data suggest that S4/D4 moves as a unit in response to depolarization, simultaneously exposing both D4:R1 and D4:R3 in WT channels.

Figure 2C also plots the scaled conductance–voltage (G–V) relationship (open diamonds) for unmodified R3C. The G–V curve, which primarily represents the voltage dependence of channel opening, is steeper than that for exposure of R3C and is shifted in a depolarizing direction, indicating that S4/D4 accounts for only part of the voltage dependence of channel opening (Yang and Horn, 1995). Presumably other voltage sensors, including the S4 segments in other domains, also contribute to activation. The kinetics of R3C exposure, like those of R1C, are very fast. The rate of modification by 100 μM MTSET was 1.23 ± 0.07 min^{-1} when a 9 s depolarization to −40 mV was applied every 20 s, or 1.45 ± 0.14 min^{-1} when 1000 depolarizations of 9 ms were alternated with 9 ms returns to the −140 mV holding potential every 20 s. These rates are not statistically different (P > .2, t test), indicating that the total duration at the depolarized voltage, not the durations of individual depolarizations, determines the modification rate, and that the exposure of R3C at −40 mV occurs in an interval much shorter than 9 ms (Yang and Horn, 1995).

Internal Accessibility of R3C and R4C

If S4 segments totally account for the voltage dependence of gating, it is not sufficient that 2 or even 3 basic residues appear and disappear on the extracellular surface, since these charged residues might always be located very close to this surface. As discussed above, it is necessary that, on the average, the equivalent of ≥2.5 charges moves completely across the membrane field in each S4 segment. Either several basic residues must each move a short distance through the electric field (e.g., Catterall, 1986; Armstrong, 1992), or else a few residues must move a large "electrical distance." To look for the latter, we put 100–200 μM MTSET into our whole-cell pipette solution to see if it could modify any of these cysteine residues from the cytoplasmic face of the protein. Although R1C was not affected by internal MTSET at any membrane potential, the inactivation kinetics of R3C and R4C were slowed by this treatment. Figures 3A and 3B show the effects of intracellular 200 μM MTSET on R3C and R4C sodium currents (compare with Figures 1B and 1C; see also Figures 1E and 1F). The kinetics of MTSET-modified R3C currents in these experiments are indistinguishable from those observed after extracellular application of this reagent. The action of intracellular MTSET started 2–5 min after obtaining the whole-cell configuration for all mutants sensitive to this reagent, suggesting that the MTSET needs time to diffuse from the patch pipette into the cell. These experiments show that at least one S4 residue, R3C,

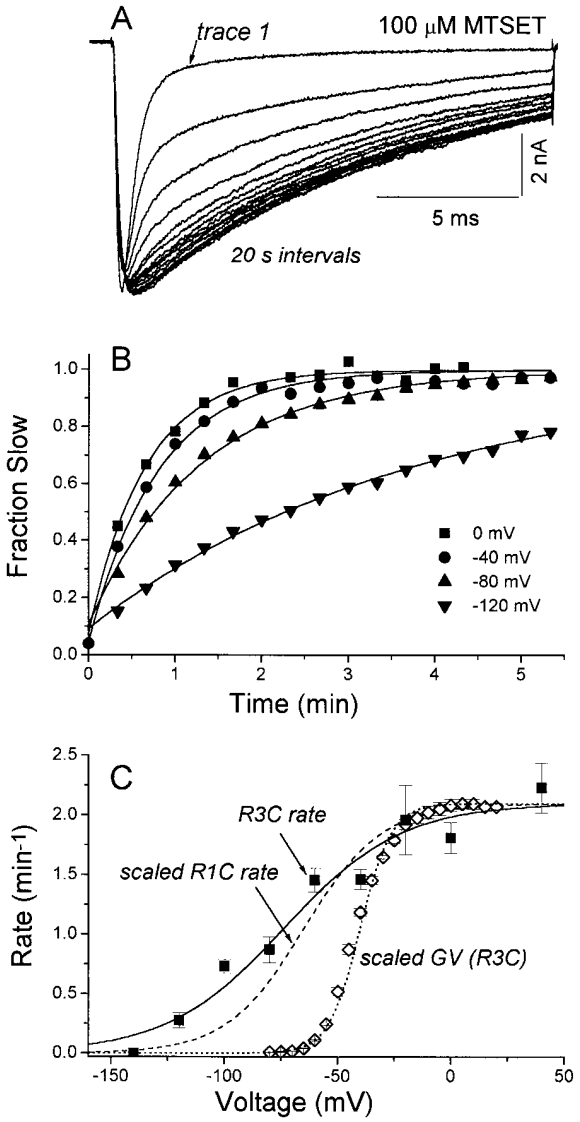

Figure 2. Kinetics and Voltage Dependence of R3C Modification by Extracellular MTSET

(A) Modification of R3C currents (same cell in Figures 1C and 1D). Depolarizations of 20 ms to −20 mV from V_{hold} = −140 mV, applied every 20 s, in the presence of 100 μM MTSET. Ten depolarizations to −20 mV (900 ms duration, each) were given in each 20 s interval between test pulses. These depolarizations cause a progressive slowing of inactivation kinetics. No modification of inactivation kinetics was observed in the absence of these depolarizations (trace 1 was obtained after 90 s exposure to MTSET, but before depolarizing the cell).

(B) Kinetics of modification of R3C currents by 100 μM MTSET. Data from 4 cells are shown, each at a different exposure voltage, applied as described in (A). A fast inactivation time constant was measured at −20 mV before exposure to MTSET, and a slow time constant was obtained after complete modification. During modification the currents were fit as a weighted sum of these 2 decaying exponentials, and the fractional weight of the slow component is plotted against time. The weights show exponential kinetics with modification time constants for these cells of 0.66 min (0 mV), 0.81 min (−40 mV), 1.30 min (−80 mV), and 3.79 min (−120 mV).

(C) The inverse of modification time constants are plotted as modification rates (closed squares). The smooth curve (solid line) is a Boltzmann relationship fit to the data with parameters given in the text. The maximum rate for the fit is 2.10 ± 0.14 min^{-1}. The dashed line shows the rate of MTSET modification of D4:R1C (Yang and Horn, 1995), scaled in amplitude and shifted to adjust for junction potential correction. The scaled peak G–V curve, obtained from the peak I–V curve for unmodified R3C, is also displayed. It is also fit by a Boltzmann function (see Table 1 for typical parameters).

can be accessible to MTSET on both the intracellular and extracellular sides of the protein.

If the appearance of R3C on the outside is dependent on depolarization, it should not be accessible intracellularly at depolarized voltages. To test this, we placed 200 μM MTSET in the patch pipette and, after obtaining the whole-cell configuration, held the cell at a depolarized voltage (−20 mV) for 10 min. This duration, at this concentration of reagent, was long enough to allow complete modification of R3C at a holding potential of −140 mV. Figure 3C shows that, after 10 min at −20 mV, R3C channels are apparently not modified, since the first current recorded after switching the holding potential to −140 mV has predominantly fast kinetics (for details, see Figure 3, legend). The modification by internal MTSET begins immediately after this change of holding potential, as shown by the progressive appearance of a slow component. This experiment excludes the possibility that internal MTSET is somehow reaching an extracellular site, since its action has the opposite voltage dependence when applied internally. Figure 3D shows, by contrast, that a 10 min depolarization to −20 mV does not protect R4C from internal MTSET, since the first current obtained after applying a −140 mV holding potential is already completely modified (i.e., there is no detectable fast component). For both R3C and R4C, the progressive increase in current amplitude in Figures 3C and 3D is due to recovery from the inactivation caused by the prolonged −20 mV holding potential. Even stronger depolarization (V_{hold} = +20 mV) failed to protect R4C from internal 200 μM MTSET (data not shown). Therefore, this residue is always accessible intracellularly.

It is not necessary to use such extreme depolarizations to inhibit the modification of R3C by intracellular MTSET. Figure 3E shows an experiment in which the holding potential was alternated between −100 and −160 mV in 1 min intervals. The individual current traces are responses to test pulses elicited at −20 mV every 20 s. The rate of modification by internal 100 μM MTSET, over this 3 min period, is markedly increased at the more negative holding voltage (Figure 3E, dashed traces). This is expected since, at −100 mV, R3C has a finite probability of being exposed outside (see Figure 2C) and therefore cannot be totally accessible internally.

To further test whether R3C can move across the protein, we modified R3C channels by depolarizing a cell in the presence of 200 μM external MTSET and attempted to remove the added -SET moiety with an intracellular hydrophilic reducing agent, tris-(2-carboxyethyl)phosphine (TCEP). TCEP (5 mM) was included in the pipette solution in these whole-cell recordings and, after modification by external MTSET, the holding potential was set at −160 mV to favor an inward position of S4/D4. Figure 3F shows that internal TCEP was capable of removing the -SET group over a period of 48 min in

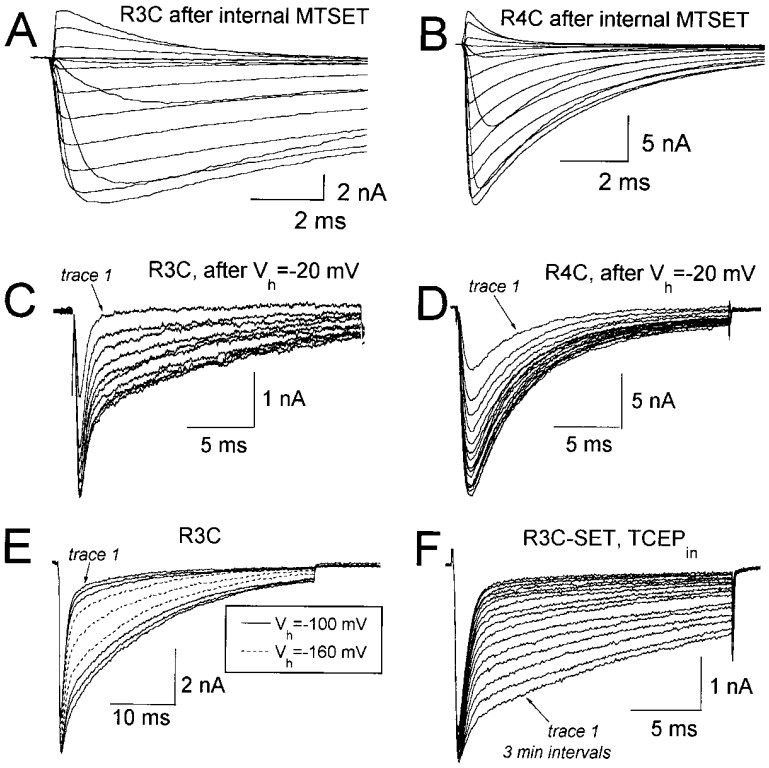

Figure 3. Effect of Intracellular MTSET on Currents of R3C and R4C

(A) and (B) show currents of R3C and R4C after modification by 200 μM MTSET in the intracellular pipette solution. $V_{hold} = -140$ mV, test pulses from −80 mV to +70 mV in 10 mV increments. The records were obtained 10–15 min after achieving the whole-cell configuration. (C) and (D) show currents obtained for test pulses to −20 mV after holding cells at −20 mV. In these experiments, 200 μM MTSET was placed in the pipette solution. After achieving whole cell and observing sodium currents, but before any noticeable effect of the MTSET, the cells were clamped at −20 mV for 10 min. Subsequently, V_{hold} was set at −140 mV, and test depolarizations to −20 mV were presented every 20 s. The initial currents (trace 1) were small in amplitude, owing to slow inactivation induced by the prolonged V_{hold} of −20 mV. The initial current of R3C had only a small slow component (fractional weight: 0.17), which could have developed in the ~10 s at −140 mV before applying the first depolarization. Over the next 3 min, the weight of the slow component grew to more than 0.60. By contrast the currents of R4C in (D) were not protected by the depolarized V_{hold}. There was no detectable fast component of the very first current, and τ_h did not change for the displayed currents. (E) shows currents of R3C in the presence of 100 μM MTSET in the pipette. Test voltage, −20 mV; V_{hold} alternated between −100 and −160 mV every minute, as indicated. The records show a consecutive series of depolarizations to −20 mV in 20 s intervals. Note that the modification is more rapid at −160 mV. Quantitatively, the fraction of the slow component increased from 0.22 to 0.35 for the first exposure to −100 mV, then up to 0.71 at −160 mV, and finally to 0.83 during the final minute at −100 mV. Similar results were obtained in 3 other cells. (F) shows effect of 5 mM TCEP, added to the intracellular pipette solution, on MTSET-modified R3C currents at $V_{hold} = -160$ mV. The MTSET was applied extracellularly at a concentration of 200 μM and removed after modification was 88% complete. The currents shown are the responses to depolarizations to −20 mV at 3 min intervals.

this experiment. The inactivation kinetics of the MTSET-modified channels did not change over this time period in the absence of TCEP (n = 3 cells), indicating the inherent stability of the introduced disulfide bond. External 5 mM TCEP, by contrast, was incapable of removing the -SET group at this negative holding potential (data not shown), confirming that TCEP is membrane impermeant. Our data show, therefore, that S4/D4 can translocate not only the R3C residue, but also the bulky, cationic -SET group, suggesting that it also translocates the WT arginine.

The direction of the voltage dependence of MTSET action on R3C cannot be explained by a model in which this cysteine residue lies in a fixed location in the membrane electric field, where it may be reached by the cationic MTSET. If this were the case, depolarization would tend to drive extracellular MTSET out of the electric field and away from the cysteine residue and therefore reduce the reaction rate. However, the voltage dependence, for both intracellular and extracellular modification, is in the opposite direction for an iontophoresis of MTSET. It is the positively charged S4 segment, not MTSET, that appears to move in response to changes of membrane potential.

Voltage-Dependent Translocation of R2C

Because R1C and R3C are both exposed extracellularly at depolarized voltages, it is likely that R2C is also exposed. If S4/D4 is an α helix, for example, all 3 of these residues would be on the same face (Figure 4A). Yet a high concentration of MTSET (500 μM) has no effect on either the fast or slow time constant of R2C inactivation at these depolarized voltages. The recovery from inactivation of R2C is significantly slowed, however, after exposure to MTSET; the recovery time constant at −140 mV, using standard two-pulse protocols (Chahine et al., 1994b), was 2.48 ± 0.06 ms for R2C and 6.85 ± 1.15 ms after exposure to 100 μM extracellular MTSET. Furthermore, this small effect on recovery depends on depolarization, suggesting that although R2C can be exposed by depolarization, the effect of extracellular MTSET is less dramatic on R2C than on R1C and R3C. We observed a similar increase in the recovery time constant in the presence of internal 100 μM MTSET, suggesting that R2C, like R3C, can traverse the hydrophobic core of the sodium channel during depolarization.

We have previously shown that the anionic reagent MTSES is capable of altering the inactivation kinetics of D4:R1C, and that depolarization is required to expose this residue to extracellular MTSES (Yang and Horn, 1995). MTSES is also capable of modifying the R2C residue, and in this case the effects are much more pronounced than we observe with MTSET. Figure 4B shows superimposed currents of R2C at a test potential of −20 mV in the absence of reagent (solid line) and in

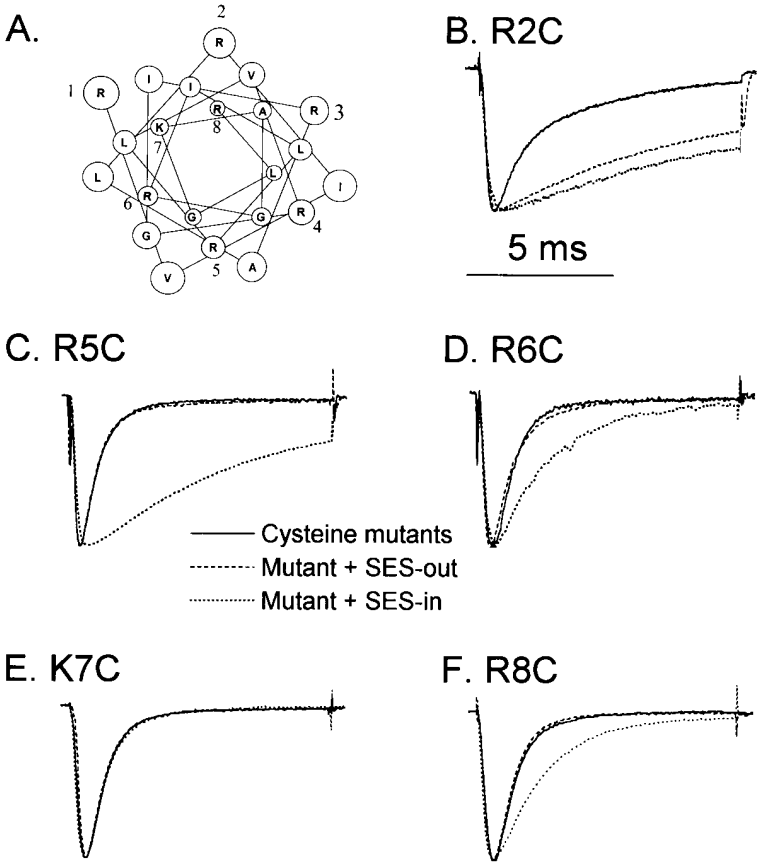

Figure 4. Accessibility of Other S4 Residues

(A) Helical wheel plot of S4/D4, showing all residues labeled by the single-letter code for amino acids. The basic residues are numbered.

(B–F) Scaled and superimposed currents (V_{test} = −20 mV; V_{hold} = −140 mV) of the indicated mutant in 3 cells, in each case after ~15 min in the whole-cell configuration. The control cell (solid lines) was not exposed to reagent. One cell was exposed to 5 mM extracellular MTSES (dashed lines), applied under depolarizing conditions (see Figure 2A). Another cell was exposed to 2 mM intracellular MTSES (dotted lines) in the patch pipette at a −140 mV holding potential for 15 min.

2 separate cells, one exposed to 5 mM extracellular MTSES (dashed line), the other exposed to 2 mM intracellular MTSES (dotted line). Depolarization was necessary to produce the kinetic effects of extracellular MTSES. These experiments indicate that R2C indeed traverses from an inwardly accessible to an outwardly accessible position during depolarization.

Accessibility of Remaining Basic S4 Residues

We have also tested the accessibility of cysteine mutants of the bottom 4 basic residues of S4/D4. Like R3C and R4C, these mutants all have rapid kinetics of inactivation in the absence of reagent (Figures 4C–4F). None of these mutants appears to react with extracellular MTSES or MTSET at any voltage, suggesting that depolarization does not expose these residues on the extracellular surface. However τ_h's of R5C, R6C, and R8C at −20 mV are significantly slowed by internal MTSES (Figures 4C–4F), which has a more pronounced effect than MTSET (data not shown). The reaction by internal reagent was not prevented by prolonged depolarizations to −20 mV for R5C showing, as for R4C, that this residue remains in an inwardly accessible position, regardless of membrane potential. Because the effects of MTSES are small on R6C and R8C, it was not possible to determine clearly whether the internal accessibilities are voltage dependent. The voltage dependence and gating kinetics of K7C were unaffected by either cysteine reagent on either external or cytoplasmic faces of the channel (Figure 4E; Table 1), suggesting either that the side chain of this residue does not face a hydrophilic compartment, or else that reaction with the cysteine reagents produces an effect too subtle to detect. K7C is the only mutant that showed no obvious reaction with cysteine reagents.

Discussion

The effects of cysteine reagents on steady-state activation and inactivation are summarized in Table 1, and the voltage-dependent accessibilities of all 8 cysteine-substituted residues are shown in Table 2. We assume that if a particular residue has an obvious reaction to a reagent from one side of the protein only (i.e., R1C, R4C, R5C, R6C, and R8C), it would also react detectably with the same reagent on the opposite side, if the residue were ever accessible there. Based on this criterion, these 5 residues are either buried in the protein or else exposed on only one face of the protein (i.e., R1C on the outside and the other four on the inside).

Our results can be summarized as follows:

First, the translocation of charge in S4/D4 may be sufficient to account for gating, since at least 2 basic residues, R2 and R3, can traverse the hydrophobic core of the channel protein. The Boltzmann curve in Figure 2C indicates the movement of 0.97 e_0 across the membrane field during R3C exposure. Because a cysteine residue, depending on its microenvironment, carries a partial negative charge (pK ≈ 8.5), and since R3C completely

Table 2. Accessibilities of S4/D4 Residues

Voltage	R1C	R2C	R3C	R4C	R5C	R6C	K7C	R8C
Hyperpolarized	buried	inside	inside	inside	inside	inside	?	inside
Depolarized	outside	outside	outside	inside	inside	not outside	?	not outside

crosses the membrane during gating, the expected charge movement for S4/D4 in a WT channel, in which an arginine is in this position, should be $\geq 2\ e_0$. Furthermore, a comparison of the voltage dependence of R1C and R3C exposure, which differ by $\sim 0.5\ e_0$ (Figure 2C), suggests that R1C moves about halfway through the membrane field. This follows because the mutation R3C, by removing a positive charge that can cross the membrane field, reduces the voltage dependence of S4/D4 movement more than R1C. Together, these data show that the outer 3 basic residues of S4/D4 are capable of translocating $\sim 2.5\ e_0$. This analysis shows not only that S4 segments could be voltage sensors underlying gating, but also that they must be the primary source of voltage dependence. If the other three S4 segments also translocate this much charge upon depolarization, then the S4 segments produce a charge transfer quantitatively close to the total charge underlying gating (Hirschberg et al., 1995). Since the total charge movement per channel is approximately equal to that which underlies gating (Sigworth, 1993), S4 segments must be the primary voltage sensors.

Second, the problem of the lack of countercharges is obviated for this S4 segment, because at most one basic residue of S4/D4 is buried within the hydrophobic core at a time.

Third, at depolarized voltages, R3C is extracellular and R4C is inside. If this section of S4/D4 is an α helix, these residues are separated by only 4.5 Å, compared with $\sim$40 Å for the bilayer thickness. If this section of S4 is more extended, these 2 residues may be $\sim$11 Å apart. In either case, the S4 charges are moving a relatively short distance across the hydrophobic core of the protein. This helps explain the ability of charges to move rapidly and reversibly. The S4 segment is acting, in effect, as a tethered permion, a sequence of charged residues whose movement across the protein is coupled with gating. The sodium channel has apparently solved the kinetics and energetics of S4 movement in the same way that many channels have solved the problem of having high selectivity and rapid permeation through an open pore (Miller, 1982), i.e., by restricting the contact region between the permeating species and its "channel." Instead of a contact region all along the S4 segment, the S4 passes through a hydrophobic "channel" or barrier that is considerably shorter than the thickness of the bilayer (Figure 5). The S4 "channel" prevents passage of these hydrophilic cysteine reagents, as well as other ionic species in the solutions bathing the protein. Because of the discrepancy between the thickness of the bilayer and the length of this hydrophobic barrier, the protein must have hydrophilic crevices or vestibules on either the external or internal surface, or both. The accessibilities of S4 residues are primarily determined by their axial positions along the segment and not by the orientation of residues around a putative α helix (e.g., see Javitch et al., 1995). This is especially clear at hyperpolarized voltages, where the residues R2C–R8C, which would wrap completely around an α helix (see Figure 4A), are all internally accessible, with the possible exception of K7C.

Figure 5 shows two possible explanations for our results; either S4 moves outward to expose its most external residues on depolarization (upper right), or else a hydrophobic portion of the protein moves inward to expose these residues (lower right). In the former case, S4 carries gating charge by moving through the electric field; in the latter case, the field moves inward past these charged residues. In either scenario charge is translocated. Although this model shows S4 segments as rather rigid structures that may move perpendicular to the plane of the membrane, it is also possible that S4 segments undergo other types of conformational reorientations, such as an uncoiling of helical regions (Guy and Conti, 1990) or a twisting of transmembrane helices (Merrill and Cramer, 1990; Unwin, 1995), in response to changes of membrane potential. Whatever the details of the conformational transitions, they must account for the changes in extracellular and intracellular accessibilities of S4 residues in response to changes of membrane potential.

Our data indicate a very short (<11 Å) hydrophobic region around S4/D4. This has three consequences worth consideration. The first is that the physical distance through which charge moves is quite short. A recent observation shows that a charged pore blocker is capable of shifting the voltage dependence of sodium channel gating as if it were repelling S4 charges electrostatically (French et al., 1996). Furthermore, this study estimated that the center of S4 charge moves $\sim$5 Å upon depolarization, consistent with the expectations of our physical model. A second consequence of the short length of the S4 "channel" is that the field strength should be substantial for typical membrane potentials ($\sim 10^8$ V/m). Although this might imply some unusual chemistry or electrostatic mechanisms due, for example, to the finite sizes of ions within such an electric field, experimental data generally do not show evidence of a breakdown in continuum electrostatic theory, even for field strengths greater than this (McLaughlin, 1989). Therefore, charge transfer can be accounted for by the electrostatically driven movement of charged S4 residues through this short "channel." The tethered connection between charged and neutral residues allows a basic residue, moving through the membrane electric field, to pull another basic residue into the S4 "channel," where it can also interact with the electric field. A final consideration is that the long side chain of an arginine residue approaches the length of the postulated S4 "channel." This raises the possibility that the distance through which the S4 backbone moves may be considerably less than that through which charged residues move.

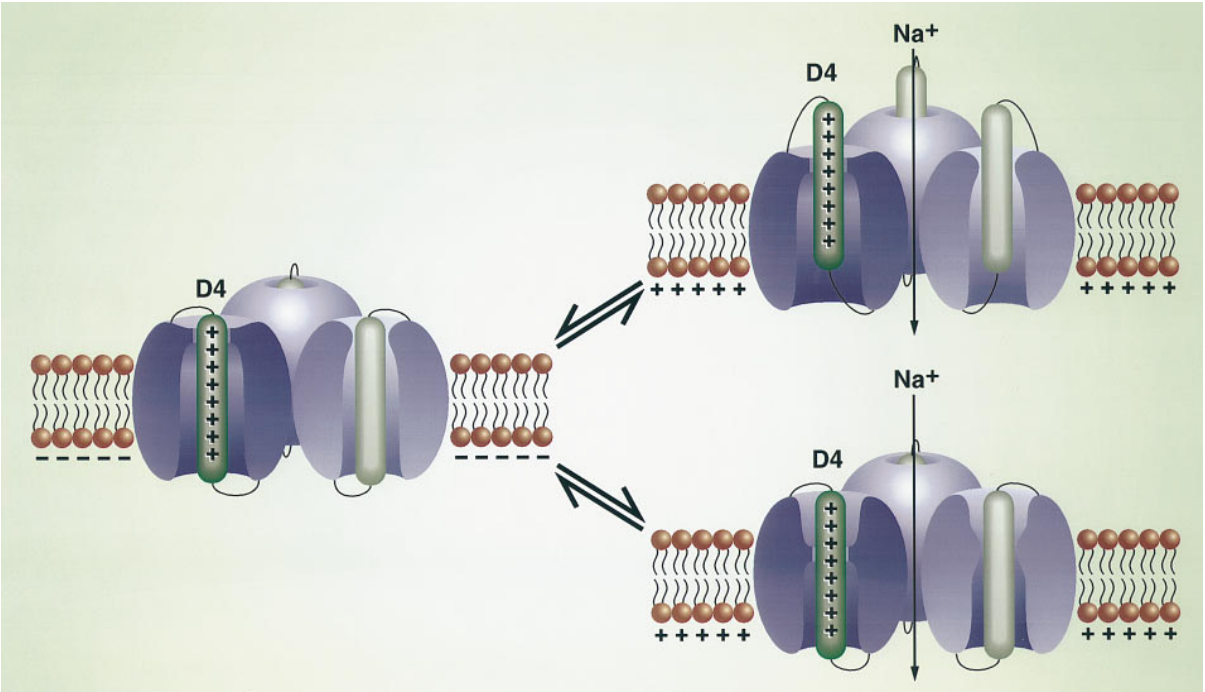

Figure 5. Models of Voltage-Dependent Exposure of S4/D4 Residues at Extracellular and Intracellular Locations

The sodium channel is oriented with extracellular surface up. The section bisects the channel through D4, another domain (presumably D2), and the ion-conducting pore. The domain in the foreground is not shown, and another domain is depicted in the background. The cartoons show dispositions of S4 residues at hyperpolarized (left) and depolarized (right) voltages. Depolarization either causes S4 to move outward (top right) or the field to move inward past it (bottom right).

Although voltage-dependent conformational changes in ion channels have been known for a long time, our data further indicate a translocation of residues across the transmembrane domain of a protein, from inwardly accessible to outwardly accessible in response to depolarization. Voltage-dependent translocations of positively charged regions of membrane proteins, or even of entire peptides, have been described previously (Martin et al., 1991; Maduke and Roise, 1993). Besides an effect on charged residues, membrane potential might also act on the dipole moment of an α helix (Tosteson et al., 1990), although it is not clear whether such an action could account for the charge movement of voltage-gated ion channels. Our data show a correlation between voltage-dependent translocation of charged residues and channel gating, as observed for an anion-selective channel from yeast (Zizi et al., 1995) and a bacterial ion channel (Slatin et al., 1994). Our studies of S4/D4 go one step further, showing that gating and translocation have approximately the same kinetics.

One of the surprising aspects of our results is that most of the charged residues in S4/D4 apparently remain in an intracellularly accessible position in spite of changes in membrane potential, indicating that they do not contribute directly to charge movement. Nevertheless, both the charged and hydrophobic residues in this portion of S4/D4 are highly conserved among sodium channel isoforms, suggesting that they play some important role in sodium channel structure or function. This role remains to be determined. By contrast to S4/D4, S4/D1 has only 4 basic residues. The outermost arginine (D1:R1), when neutralized to glutamine, has almost no effect on either activation or inactivation (Stühmer et al., 1989; Chen et al., 1995, Biophys. J., abstract). Therefore, it is likely that the remaining 3 basic residues in S4/D1 are all involved in voltage sensing, consistent with mutagenic studies (Stühmer et al., 1989; Chen et al., 1995, Biophys. J., abstract).

Although we focus on S4 segments primarily as activation voltage sensors, the greatest effects of the cysteine reagents in our experiments are on the rate of inactivation. In fact, the ability to explore the detailed voltage-dependent accessibility of S4 residues depends critically on the dramatic effects on τ_h. S4/D4 plays a unique role in the process of inactivation, a role not played by S4 segments in other domains (Chen et al., 1995, Biophys. J., abstract). By contrast, all S4 segments contribute to activation (Chen et al., 1995, Biophys. J., abstract). We can only speculate on the mechanisms by which the cysteine reagents affect inactivation, either decreasing τ_h (R1C) or increasing it (all others). If outward movement of S4/D4 enhances entry into an inactivated state, then the modification of R1C by MTSET may tend to favor an outward conformation, whereas reaction with the other S4/D4 residues tends to keep the segment in an inward conformation. These postulated alterations in S4/D4 mobility also affect activation (e.g., Table 1), but the effects are more subtle, perhaps because other S4 segments also contribute strongly to activation.

If S4 residues enter a vestibule when they move outward (Figure 5), and if the extracellular mouth of the pore of an ion channel also consists of a vestibule, we can ask whether they share the same vestibule and how close they are. We address this by testing whether an

extracellular pore blocker can prevent modification of an S4 residue by MTSET. Saturating concentrations of either tetrodotoxin (3 μM) or the larger blocker μ-conotoxin (6 μM; IC_{50} = 1.2 μM; Chahine et al., 1994a) each fail to prevent the reaction between extracellular 20 μM MTSET and D4:R1C, showing that R1C emerges outside of the footprint of μ-conotoxin, which has a radius of ~6 Å (Lancelin et al., 1991; Chahine et al., 1995). These data indicate that the S4 "channel" is distinct from the ion-conducting pore.

Experimental Procedures

Mutagenesis

Site-directed mutagenesis was performed either using the Altered Sites mutagenesis system employing the plasmid vector pSELECT (Promega Corp., Madison, WI) as previously described (Chahine et al., 1994b), or by using the overlap-extension polymerase chain reaction (PCR) mutagenesis method (Higuchi, 1989). Mutations R1451C (R2C), R1454C (R3C), and R1457C (R4C) were made using the pSELECT system with the following mutagenic oligonucleotides:

R2C, 5′-CCGCGCCAGGCAGATCACACGGA-3′;

R3C, 5′-GACACGCCCAATGCACGCCAGGCGGAT-3′;

R4C, 5′-CCGCAGGACACACCCAATCCGCG-3′.

These mutations were verified by dideoxynucleotide sequencing before assembling full-length mutant hSkM1 constructs in the mammalian expression vector pRc/CMV. Mutant R1448C (R1C) was constructed as previously described (Chahine et al., 1994b).

The following mutations were made in hSkM1 using PCR mutagenesis: R1460C (R5C), R1463C (R6C), K1466C (K7C), and R1469C (R8C). Final products were digested with BstEII and ClaI to produce a 437 bp fragment that was directionally cloned into the full-length pRc/CMV-hSkM1 construct. Recombinants were sequenced to verify the mutation and to exclude polymerase errors in the amplified 437 bp region.

All mutant constructs were introduced into tsA201 cells by transient transfection (Chahine et al., 1994b). Cells were used for recording 40–80 hr after transfection.

Electrophysiology and Data Acquisition

Standard whole-cell recording methods were used as previously described (Yang and Horn, 1995). Supercharging reduced the expected charging time constant for the cells to <4.0 μs. Series resistance errors were <3 mV. Data were filtered at 5 kHz and acquired using pCLAMP (Axon Instruments, Burlingame, CA). Patch electrodes contained 105 mM CsF, 35 mM NaCl, 10 mM EGTA, 10 mM Cs-HEPES (pH 7.4). The bath contained 150 mM NaCl, 2 mM KCl, 1.5 mM $CaCl_2$, 1 mM $MgCl_2$, and 10 mM Na-HEPES (pH 7.4). Corrections were made for liquid junction potentials. All experiments were performed at 18°C.

Whole-cell data were analyzed and displayed by a combination of pCLAMP programs, ORIGIN (MicroCal, Northampton, MA), and our own FORTRAN programs. Data from at least 3 cells for each measurement are presented as mean ± SEM. Steady-state inactivation was measured by reduction in peak current at −20 mV preceded by a 500 ms conditioning pulse. To obtain the statistics in Table 1, which are parameters for a Boltzmann function, we fit data from individual cells; the statistics presented are mean ± SEM for these best-fit parameters.

MTSET and MTSES were generous gifts from Rolf Joho and Arthur Karlin. The cationic MTSET covalently attaches ethyl-trimethylammonium to the reduced cysteine sulfhydryl via a disulfide bond, and the anionic MTSES attaches ethyl-sulfonate. Aqueous stocks of these reagents were kept at 4°C and diluted in the bath solution immediately before use. The reagent solutions were loaded into a large-bore sigmacoted (Sigma, St. Louis, MO) macropipette, the opening of which was placed in apposition to the cell voltage clamped by a patch pipette. The macropipette diameter was 1–10× that of the cell (~15 μm), and the opening was <50 μm from the cell. The cells were usually maintained at a holding potential (V_{hold}) of −140 mV and stimulated every 20 s by a 20 ms test pulse to −20 mV, to measure inactivation kinetics. Effects of these reagents were irreversible in the absence of added reducing agents. Although WT channels have >12 cysteines on both extracellular and cytoplasmic surfaces, according to standard topological representations of the folding of transmembrane segments, neither MTS reagent had an effect on WT channels. This is demonstrated clearly in Figure 4, where various mutants fail to respond to either internal or external MTSES. In some experiments, 5 mM TCEP (Molecular Probes, Eugene, OR) was added to either the intracellular pipette solution or the extracellular bath solution. These solutions were titrated to pH 7.4 with either CsOH (pipette solution) or NaOH (bath solution).

Depolarizations were required for extracellular exposure of S4 residues. Except where indicated otherwise, 10 depolarizations of 900 ms each were presented in the 20 s interval between brief test depolarizations. Between each of these 10 depolarizations, the voltage was returned to −140 mV for 900 ms. Therefore, the cells spent a total of 9 s at a depolarized potential and 11 s at −140 mV between each test depolarization. In one series of experiments, we applied a single 9 s depolarization to −40 mV every 20 s; and in another series, we applied 1000 depolarizations of 9 ms each to −40 mV, to test the kinetics of cysteine exposure (Yang and Horn, 1995).

Acknowledgments

We thank Drs. Michael O'Leary and Carol Deutsch for helpful discussions and comments on the manuscript, Dr. Fred Sigworth for insightful discussions, and Aaron Benson and Vincent Santarelli for technical assistance with mutagenesis and tissue culture. Supported by National Institutes of Health grants AR41691 (R. H.) and NS32387 (A. L. G.). A. L. G. is a Lucille P. Markey Scholar.

The costs of publication of this article were defrayed in part by the payment of page charges. This article must therefore be hereby marked *"advertisement"* in accordance with 18 USC Section 1734 solely to indicate this fact.

Received November 16, 1995; revised November 28, 1995.

References

Akabas, M.H., Stauffer, D.A., Xu, M., and Karlin, A. (1992). Acetylcholine receptor channel structure probed in cysteine-substitution mutants. Science *258*, 307–310.

Armstrong, C.M. (1992). Voltage-dependent ion channels and their gating. Physiol. Rev. *72* (Suppl.), S5–S13.

Auld, V.J., Goldin, A.L., Krafte, D.S., Catterall, W.A., Lester, H.A., Davidson, N., and Dunn, R.J. (1990). A neutral amino acid change in segment IIS4 dramatically alters the gating properties of the voltage-dependent sodium channel. Proc. Natl. Acad. Sci. USA *87*, 323–327.

Catterall, W.A. (1986). Molecular properties of voltage-sensitive sodium channels. Annu. Rev. Biochem. *55*, 953–985.

Chahine, M., Bennett, P.B., George, A.L., Jr., and Horn, R. (1994a). Functional expression and properties of the human skeletal muscle sodium channel. Pflügers. Arch. *427*, 136–142.

Chahine, M., George, A.L., Jr., Zhou, M., Ji, S., Sun, W., Barchi, R.L., and Horn, R. (1994b). Sodium channel mutations in paramyotonia congenita uncouple inactivation from activation. Neuron *12*, 281–294.

Chahine, M., Chen, L.-Q., Fotouhi, N., Walsky, R., Fry, D., Santarelli, V., Horn, R., and Kallen, R.G. (1995). Characterizing the μ-conotoxin binding site on voltage-sensitive sodium channels with toxin analogs and channel mutations. Recept. Channels, *3*, 161–174.

Durell, S.R., and Guy, H.R. (1992). Atomic scale structure and functional models of voltage-gated potassium channels. Biophys. J. *62*, 238–247.

Fleig, A., Fitch, J.M., Goldin, A.L., Rayner, M.D., Starkus, J.G., and Ruben, P.C. (1994). Point mutations in IIS4 alter activation and inactivation of rat brain IIA Na channels in *Xenopus* oocyte macropatches. Pflügers Arch. *427*, 406–413.

French, R.J., Prusak-Sochaczewski, E., Zamponi, G.W., Becker, S., Shavantha Kularatna, A., and Horn, R. (1996). Electrostatic interactions between a pore-blocking peptide and the voltage sensor of a sodium channel—a novel approach to channel geometry. Neuron, in press.

George, A.L., Jr., Komisarof, J., Kallen, R.G., and Barchi, R.L. (1992). Primary structure of the adult human skeletal muscle voltage-dependent sodium channel. Ann. Neurol. *31*, 131–137.

Guy, H.R., and Conti, F. (1990). Pursuing the structure and function of voltage-gated channels. Trends Neurosci. *13*, 201–206.

Higuchi, R. (1989). Using PCR to engineer DNA. In PCR Technology, H.A. Erlich, ed. (New York: Stockton Press), pp. 61–70.

Hirschberg, B., Rovner, A., Lieberman, M., and Patlak, J. (1995). Transfer of twelve charges is needed to open skeletal muscle Na channels. J. Gen. Physiol., in press.

Javitch, J.A., Fu, D., Chen, J., and Karlin, A. (1995). Mapping the binding-site crevice of the dopamine D2 receptor by the substituted-cysteine accessibility method. Neuron *14*, 825–831.

Lancelin, J.M., Kohda, D., Tate, S., Yanagawa, Y., Abe, T., Satake, M., and Inagaki, F. (1991). Tertiary structure of conotoxin GIIIA in aqueous solution. Biochemistry *30*, 6908–6916.

Liman, E.R., Hess, P., Weaver, F., and Koren, G. (1991). Voltage-sensing residues in the S4 region of a mammalian K^+ channel. Nature *353*, 752–756.

Logothetis, D.E., Movahedi, S., Satler, C., Lindpaintner, K., and Nadal-Ginard, B. (1992). Incremental reductions of positive charge within the S4 region of a voltage-gated K^+ channel result in corresponding decreases in gating charge. Neuron *8*, 531–540.

Logothetis, D.E., Kammen, B.F., Lindpaintner, K., Bisbas, D., and Nadal-Ginard, B. (1993). Gating charge differences between two voltage-gated K^+ channels are due to the specific charge content of their respective S4 regions. Neuron *10*, 1121–1129.

Lopez, G.A., Jan, Y.N., and Jan, L.Y. (1991). Hydrophobic substitution mutations in the S4 sequence alter voltage-dependent gating in *Shaker* K^+ channels. Neuron *7*, 327–336.

Maduke, M., and Roise, D. (1993). Import of a mitochondrial presequence into protein-free phospholipid vesicles. Science *260*, 364–367.

Martin, J., Mahlke, K., and Pfanner, N. (1991). Role of an energized inner membrane in mitochondrial protein import. $\Delta\psi$ drives the movement of presequences. J. Biol. Chem. *266*, 18051–18057.

McCormack, K., Tanouye, M.A., Iverson, L.E., Lin, J.-W., Ramaswami, M., McCormack, T., Campanelli, J.T., Mathew, M.K., and Rudy, B. (1991). A role for hydrophobic residues in the voltage-dependent gating of Shaker K^+ channels. Proc. Natl. Acad. Sci. USA *88*, 2931–2935.

McLaughlin, S. (1989). The electrostatic properties of membranes. Annu. Rev. Biophys. Biophys. Chem. *18*, 113–136.

Merrill, A.R., and Cramer, W.A. (1990). Identification of a voltage-responsive segment of the potential-gated colicin E1 ion channel. Biochemistry *29*, 8529–8534.

Miller, C. (1982). Feeling around inside a channel in the dark. In Transport in Biological Membranes, R. Antolini, ed. (New York: Raven), pp. 99–108.

Noda, M., Shimizu, S., Tanabe, T., Takai, T., Kayano, T., Ikeda, T., Takahashi, H., Nakayama, H., Kanaoka, Y., Minamino, N., et al. (1984). Primary structure of *Electrophorus electricus* sodium channel deduced from cDNA sequence. Nature *312*, 121–127.

Papazian, D.M., Timpe, L.C., Jan, Y.N., and Jan, L.Y. (1991). Alteration of voltage-dependence of Shaker potassium channel by mutations in the S4 sequence. Nature *349*, 305–310.

Papazian, D.M., Shao, X.M., Seoh, S.-A., Mock, A.F., Huang, Y., and Wainstock, D.H. (1995). Electrostatic interactions of S4 voltage sensor in Shaker K^+ channel. Neuron *14*, 1293–1301.

Perozo, E., Santacruz-Toloza, L., Stefani, E., Bezanilla, F., and Papazian, D.M. (1994). S4 mutations alter gating currents of Shaker K channels. Biophys. J. *66*, 345–354.

Schoppa, N.E., McCormack, K., Tanouye, M.A., and Sigworth, F.J. (1992). The size of gating charge in wild-type and mutant Shaker potassium channels. Science *255*, 1712–1715.

Sigworth, F.J. (1993). Voltage gating of ion channels. Quart. Rev. Biophys. *27*, 1–40.

Slatin, S.L., Qiu, X.-Q., Jakes, K.S., and Finkelstein, A. (1994). Identification of a translocated protein segment in a voltage-dependent channel. Nature *371*, 158–161.

Stauffer, D.A., and Karlin, A. (1994). Electrostatic potential of the acetylcholine binding sites in the nicotinic receptor probed by reactions of binding-site cysteines with charged methanethiosulfonates. Biochemistry *33*, 6840–6849.

Stühmer, W., Conti, F., Suzuki, H., Wang, X., Noda, M., Yahagi, N., Kubo, H., and Numa, S. (1989). Structural parts involved in activation and inactivation of the sodium channel. Nature *339*, 597–603.

Tosteson, M.T., Alvarez, O., Hubbell, W., Bieganski, R.M., Attenbach, C., Levy, J.J., Nutt, R.F., Rosenblatt, M., and Tosteson, D.C. (1990). Primary structure of peptides and ion channels. Role of amino acid side chains in voltage gating of melittin channels. Biophys. J. *58*, 1367–1375.

Unwin, N. (1995). Acetylcholine receptor channel imaged in the open state. Nature *373*, 37–43.

Yang, N., and Horn, R. (1995). Evidence for voltage-dependent S4 movement in sodium channels. Neuron *15*, 213–218.

Zagotta, W.N., Hoshi, T., Dittman, J., and Aldrich, R.W. (1994). *Shaker* potassium channel gating. II. Transitions in the activation pathway. J. Gen. Physiol. *103*, 279–319.

Zizi, M., Thomas, L., Blachly-Dyson, E., Forte, M., and Colombini, M. (1995). Oriented channel insertion reveals the motion of a transmembrane β strand during voltage gating of VDAC. J. Memb. Biol. *144*, 121–129.